arXiv:astro-ph/9901108v1 10 Jan 1999

Accretion Disk Models

Andrei M. Beloborodov[1]

Stockholm Observatory, Saltsjöbaden, S-133 36, Sweden

Abstract. Models of black hole accretion disks are reviewed, with an emphasis on the theory of hard X-ray production. The following models are considered: i) standard, ii) super-critical, iii) two-temperature, and iv) disk+corona. New developments have recently been made in hydrodynamical models of accretion and in phenomenological radiative models fitting the observed X-ray spectra. Attempts to unify the two approaches are only partly successful.

1. Introduction

Accretion disks around black holes are efficient radiators which can convert a sizable fraction of gas rest mass energy into radiation. The disk forms if the specific angular momentum of the accreting gas $j \gg r_g c$, where $r_g = 2GM/c^2$ is the gravitational radius of the black hole. Then the radial infall is stopped by the centrifugal potential barrier at a radius $r_d \sim j^2/r_g c^2$, the gas cools and forms a ring rotating with Keplerian velocity. Further accretion is possible only if some mechanism redistributes angular momentum, allowing gas to spiral toward the black hole. A plausible mechanism is provided by MHD turbulence that develops due to the differential character of Keplerian rotation (see Balbus & Hawley 1998 for a review). Turbulent pulsations force each gas element to diffuse from one Keplerian orbit to another, and a ring of gas spreads out to form an extended disk. At the inner edge of the disk gas is absorbed by the black hole. The diffusion problem with the absorbing inner boundary has stationary solutions, each specified by a net accretion rate, $\dot{M}$. The redistribution of angular momentum is accompanied by a viscous heating. As a result, the binding energy of spiraling gas is dissipated into heat and can be radiated.

In this review, we concentrate on steady disk models and their applications to active galactic nuclei (AGNs) and galactic black hole candidates (GBHs). Observed spectra of the black hole sources indicate that accretion disks usually do *not* radiate as a blackbody. In particular, a huge luminosity comes out in hard X-rays. The origin of the hard X-ray component has been in the focus of interest since the component was detected, and it remains as a challenge for theoretical models of accretion disks. We start with the standard disk model (Section 2) and then discuss the concept of advective disks (Section 3). In Section 4, we

[1]Also at Astro-Space Center of Lebedev Physical Institute, Profsoyuznaya 84/32, 117810 Moscow, Russia

discuss super-critical disk models. In Section 5, two-temperature models are reviewed. Finally, in Section 6, we summarize new developments concerning the disk-corona model.

2. The standard model

The standard model (see Pringle 1981 for a review) provides a commonly used simple description of an accretion disk. The model considers a thin gaseous disk of surface density Σ and density $\rho = \Sigma/2H$, where H is the disk height-scale. The disk rotates around the black hole with a Keplerian angular velocity, $\Omega_{\rm K} = (GM/r^3)^{1/2}$. H is regulated by the pressure in the disk, p, which supports the gas against the vertical component of gravity. The vertical balance reads

$$\frac{H}{r} = \frac{c_s}{v_{\rm K}}, \tag{1}$$

where $c_s^2 \equiv p/\rho$ and $v_{\rm K} = \Omega_{\rm K} r$. The matter in the disk gradually drifts inward due to a viscous stress $t_{r\varphi} = \nu\rho r(\mathrm{d}\Omega_{\rm K}/\mathrm{d}r)$ where ν is a kinematic viscosity coefficient. The stress is a fraction of the pressure, $t_{r\varphi} = \alpha p$, where $\alpha < 1$ is assumed to be constant (Shakura 1972). Equivalently, $\nu = (2/3)\alpha c_s H$. The inward drift is governed by the angular momentum equation,

$$vr\Sigma\frac{\mathrm{d}}{\mathrm{d}r}(\Omega_{\rm K} r^2) = \frac{\mathrm{d}}{\mathrm{d}r}(T_{r\varphi} r^2), \qquad T_{r\varphi} \equiv 2Ht_{r\varphi} = \frac{3}{2}\nu\Sigma\Omega_{\rm K}. \tag{2}$$

Here v is the accretion velocity. In a steady disk,

$$2\pi r v \Sigma = \dot{M} = const, \tag{3}$$

which allows the angular momentum equation to be integrated,

$$T_{r\varphi} = \frac{\dot{M}\Omega_{\rm K}}{2\pi}\left(1 - \frac{C}{\sqrt{r}}\right). \tag{4}$$

The constant C is determined by an inner boundary condition. In the very vicinity of the black hole, Keplerian rotation becomes unstable and gas falls into the black hole with a constant angular momentum. The radius of the marginally stable Keplerian orbit is $r_{\rm ms} = 3r_g$ for a Schwarzschild black hole. The standard model treats the transition to free fall by placing the inner disk boundary at $r_{\rm in} = r_{\rm ms}$ and by assuming $t_{r\varphi} = 0$ at $r = r_{\rm in}$. Then $C = \sqrt{3r_g}$.

The accretion velocity may be expressed from (3) and (4) as

$$v = \frac{3}{2}\frac{\nu}{r}S^{-1} = \alpha\frac{c_s^2}{v_{\rm K}}S^{-1}, \qquad S \equiv 1 - \left(\frac{3r_g}{r}\right)^{1/2}. \tag{5}$$

The viscous heating rate (per unit area of the disk) is

$$F^+ = T_{r\varphi} r\frac{\mathrm{d}\Omega_{\rm K}}{\mathrm{d}r} = \frac{3}{2}T_{r\varphi}\Omega_{\rm K} = \frac{3\dot{M}}{4\pi}\Omega_{\rm K}^2 S. \tag{6}$$

The standard model assumes that the bulk of the dissipated energy is radiated away locally, i.e., the local heating rate, F^+, is balanced by the radiative losses from the two faces of the disk, $2F = F^-$. The disk therefore remains cold and thin, $c_s \ll v_{\rm K}$, $H \ll r$, and accretion is slow, $v \ll v_{\rm K}$.

As the binding energy is radiated away, the radiative efficiency of accretion is $\eta = b_{\rm in}/c^2$, where $b_{\rm in}$ is the specific binding energy at the inner edge. In the simplest version (eqs. [1-6]), a Newtonian gravitational field is assumed, with the potential GM/r. Then $b_{\rm in} = GM/2r_{\rm in} = c^2/12$. A relativistic version (Novikov & Thorne 1973; Page & Thorne 1974) yields $0.06 < \eta < 0.42$ depending on the black hole spin. The highest efficiency is achieved for a maximally rotating black hole. Then the stable Keplerian disk spreads deep into the potential well, $r_{\rm ms} \to r_g/2$, and this results in a high binding energy at the inner edge, $b_{\rm in} = c^2(1 - 1/\sqrt{3}) \approx 0.42c^2$.

The set of disk structure equations (1), (3), (5), and (6) should be completed by an equation of state and an equation specifying a mechanism of radiative cooling. In particular, if (i) the pressure in the disk is dominated by ionized gas with a temperature T, so that $c_s^2 \approx 2kT/m_p$, and (ii) the produced radiation is near thermodynamic equilibrium with the gas and gradually diffuses out of the disk, then $F \approx ca_rT^4/\sqrt{3}\tau = (ca_rm_p^4/16\sqrt{3}k^4)c_s^8/\tau$, where $a_r = 7.56 \times 10^{-15}$ is the radiation constant and $2\tau = \sigma_{\rm T}\Sigma/m_p$ is the Thomson optical depth across the disk. It completes the set of equations and the disk parameters can be expressed as analytical functions of radius, each model being specified by $\dot{M}$ and α (Shakura & Sunyaev 1973). We will hereafter express $\dot{M}$ in a dimensionless form, $\dot{m} = \dot{M}c^2/L_{\rm E}$, where $L_{\rm E} = 2\pi r_g m_p c^3/\sigma_{\rm T}$ is the Eddington luminosity.

When $\dot{m}$ exceeds $\sim 0.1(\alpha M/M_\odot)^{-1/8}$ there appears a region in the disk where the radiation pressure dominates the gas pressure. Then the disk thickness is determined by the vertical radiation flux, $GMm_pH/r^3 = F\sigma_{\rm T}/c$, and the set of equations may be closed by the condition $H = (3/4)\dot{m}r_gS$. The model then becomes viscously (Lightman & Eardley 1974) and thermally (Shakura & Sunyaev 1976) unstable. The instabilities are reviewed by Julian Krolik in these proceedings.

Assuming that the disk radiates as a black body, $F = \sigma T_*^4$, one gets

$$T_* \approx 3.5 \times 10^7 \dot{m}^{1/4} \left(\frac{M}{M_\odot}\right)^{-1/4} \left(\frac{r}{r_g}\right)^{-3/4} S^{1/4}. \qquad (7)$$

A maximum surface temperature is $T_* \sim 10^5$ K for AGNs ($M \sim 10^7 - 10^9 M_\odot$) and $T_* \sim 10^7$ K for GBHs ($M \sim 10 M_\odot$). It is the major success of the model that T_* approximately corresponds to observed UV emission in AGNs and X-ray emission in GBHs. The hard X-ray component would, however, correspond to a temperature $\sim 10^9$ K. The standard model may yield such high temperatures only if the accretion rate is near the critical value, $\dot{m}_{\rm cr} = \eta^{-1}$, that corresponds to the critical Eddington luminosity. Near-critical disks can strongly deviate from the blackbody state provided α is large (Shakura & Sunyaev 1973). An overheating then occurs in the inner region of the disk where the inflow time-scale is shorter than the time-scale for relaxation to thermodynamic equilibrium. This effect is discussed in more detail in Section 4.

3. Advective disks: basic equations

The key assumption of the standard model, that the dissipated energy is radiated away locally, is relaxed in the presently popular models of advection-dominated accretion flows (ADAFs, see Narayan, Mahadevan & Quataert 1998 for a review). There are two types of ADAFs: super-critical (see Section 4) and two-temperature (see Section 5.2). In both models, a large fraction of the released energy is stored in the gas and advected into the black hole instead of being radiated away. Advective disks are geometrically thick, and a two-dimensional (2D) approach would be more adequate to the problem. Most of the models are, however, based on the vertically integrated (1D) equations due to their simplicity. The α-parametrization of viscosity is used in the same manner as in the standard model, sometimes with modifications suppressing α at the sonic radius to avoid the causality problem (Narayan 1992). By solving the 1D equations, one gets typical parameters of the accreting gas as a function of radius.

Advection implies a non-local character of the flow, so that one deals with a set of non-linear differential equations with boundary conditions. In the innermost region, the flow passes through a sonic radius, r_s, where the radial velocity v exceeds the sound speed. A regularity condition must be fulfilled for any steady transonic flow at $r = r_s$ (cf. Landau & Lifshitz 1987). This condition reads $N = D = 0$ where N and D are the numerator and denominator in the explicit expression for the derivative $\mathrm{d}v/\mathrm{d}r$. The regularity condition gives two extra equations that determine r_s and impose a connection between $\dot{M}$ and the flow parameters at an external boundary.

The transonic character of accretion is related to a special feature of a black hole gravitational field: the effective potential for radial motion with a given angular momentum has a maximum (see Misner, Thorne & Wheeler 1973). After passing the potential barrier, rotation cannot stop the inflow. The relativistic nature of a black hole gravitational field can be approximately described by the pseudo-Newtonian potential $\varphi = GM/(r - r_g)$ (Paczyński & Wiita 1980) which is a good approximation for a Schwarzschild black hole. Similar potentials have been proposed to emulate the gravitational field of a rotating black hole (Artemova, Björnsson & Novikov 1996). The pseudo-Newtonian models were studied by Paczyński & Bisnovatyi-Kogan (1981) and in many subsequent works. Recently, fully relativistic 1D equations have been derived (Lasota 1994; Abramowicz et al. 1996). We here summarize the relativistic equations with some corrections (Beloborodov, Abramowicz & Novikov 1997).

First, we summarize notation. The Kerr geometry is described by the metric tensor g_{ij} in the Boyer-Lindquist coordinates $x^i = (t, r, \theta, \varphi)$ (given, e.g., in Misner et al. 1973). The four-velocity of the accreting gas is $u^i = (u^t, u^r, u^\theta, u^\varphi)$ with $u^\theta = 0$ assumed in the 1D model. The angular velocity of the gas is $\Omega = u^\varphi/u^t$ and its Lorentz factor is $\gamma = u^t(-g^{tt})^{-1/2}$ measured in the frame of local observers having zero angular momentum. The vertically integrated parameters of the disk are: surface rest mass density Σ, surface energy density $U = \Sigma c^2 + \Pi$ (Π being the internal energy), and the vertically integrated pressure P. The dimensionless specific enthalpy is $\mu = (U + P)/\Sigma c^2$. F^+ is the rate of viscous heating, and F^- is the local radiation flux from the two faces of the disk. Σ, U, Π, P, and $F^\pm$ are measured in the local comoving frame.

The main equations of a steady disk express the general conservation laws discussed by Novikov & Thorne (1973) and Page & Thorne (1974) in the context of the standard model. For advective disks, the assumption $\Omega = \Omega_{\rm K}^{+}$ is replaced by the radial momentum equation, and the assumption $F^{+} = F^{-}$ is replaced by the energy equation including the advection term.

Mass conservation: $$2\pi r c u^{r} \Sigma = -\dot{M}$$

Angular momentum: $$\frac{\mathrm{d}}{\mathrm{d}r}\left[\mu\left(\frac{\dot{M}u_{\varphi}}{2\pi} + 2\nu\Sigma r \sigma^{r}{}_{\varphi}\right)\right] = \frac{F^{-}}{c^{2}}\, r u_{\varphi},$$

where $$\sigma^{r}{}_{\varphi} = \frac{1}{2}\, g^{rr} g_{\varphi\varphi} \sqrt{-g^{tt}}\, \gamma^{3} \frac{\mathrm{d}\Omega}{\mathrm{d}r}$$ is the shear.

Energy: $$F^{+} - F^{-} = c u^{r} \left(\frac{\mathrm{d}\Pi}{\mathrm{d}r} - \frac{\Pi + P}{\Sigma}\frac{\mathrm{d}\Sigma}{\mathrm{d}r}\right),$$

where $$F^{+} = \nu\Sigma\mu c^{2} g^{rr} g_{\varphi\varphi}\left(-g^{tt}\right)\gamma^{4}\left(\frac{\mathrm{d}\Omega}{\mathrm{d}r}\right)^{2}.$$

Radial momentum: $$\frac{1}{2}\,\frac{\mathrm{d}}{\mathrm{d}r}\left(u_{r}u^{r}\right) = -\frac{1}{2}\,\frac{\partial g_{\varphi\varphi}}{\partial r} g^{tt}\gamma^{2}\left(\Omega - \Omega_{\rm K}^{+}\right)\left(\Omega - \Omega_{\rm K}^{-}\right) - \frac{1}{c^{2}\Sigma\mu}\frac{\mathrm{d}P}{\mathrm{d}r} - \frac{F^{+}u_{r}}{c^{3}\Sigma\mu},$$

where $\Omega_{\rm K}^{\pm}$ are Keplerian angular velocities for the co-rotating (+) and counter-rotating (−) orbits

$$\Omega_{\rm K}^{\pm} = \pm\frac{c}{r(2r/r_{g})^{1/2} \pm a_{*} r_{g}/2}.$$

Here $a_{*} \leq 1$ is the spin parameter of the black hole.

The set of disk structure equations gets closed when the viscosity ν, the equation of state $P(\Pi)$, and the radiative cooling F^{-} are specified. A standard prescription for viscosity is $\nu = \alpha c_{s} H$, where α is a constant and $c_{s} = c(P/U)^{1/2}$ is the isothermal sound speed. The half-thickness of the disk, H, should be estimated from the vertical balance condition. Near the black hole, the tidal force compressing the disk in vertical direction depends on Ω (e.g., Abramowicz, Lanza & Percival 1997). For $\Omega \approx \Omega_{K}^{+}$, which is a good approximation for the vertical balance, one gets (e.g., Riffert & Herold 1995)

$$H^{2} = \frac{P}{U}\,\frac{2r^{3}}{r_{g}J}, \qquad \text{where} \qquad J(a_{*}, r) = \frac{2(r^{2} - a_{*} r_{g}\sqrt{2r_{g}r} + 0.75 a_{*}^{2} r_{g}^{2})}{2r^{2} - 3r_{g}r + a_{*} r_{g}\sqrt{2r_{g}r}}$$

is a relativistic correction factor becoming unity at $r \gg r_g$.

The disk luminosity is related to $\dot{M}$ by (Beloborodov et al. 1997)

$$L^- = -\frac{2\pi}{c}\int\limits_{r_s}^{\infty} u_t F^- r \mathrm{d}r \approx \dot{M}c^2\left(1+\mu_{\rm in}\frac{u_t^{\rm in}}{c}\right),$$

where the index "in" refers to the inner transonic edge of the disk, in particular, $\mu_{\rm in}$ is the dimensionless specific enpthalpy at the inner edge. The radiative efficiency of the disk equals

$$\eta = \frac{L^-}{\dot{M}c^2} = 1-\mu_{\rm in}\left(1-\frac{b_{\rm in}}{c^2}\right). \qquad (8)$$

Here, $b_{\rm in} = c^2 + u_t^{\rm in}c$ is the specific binding energy at the inner edge. In the standard model, $\mu_{\rm in}=1$ and $\eta = b_{\rm in}/c^2$. In the advective limit $\eta \to 0$, and hence $\mu_{\rm in} \to (1-b_{\rm in}/c^2)^{-1}$. Note that one should not assume $b_{\rm in}=0$ for advective disks. In fact, the position and binding energy of the inner edge can be found only by integrating the disk structure equations. The difference $\mu_{\rm in}-1$ (which describes the relativistic increase of gas inertia due to stored heat) adjusts to keep $\eta \approx 0$.

4. Super-critical disks

Large accretion rates are expected in the brightest objects, such as quasars or transient GBHs during outbursts. When the accretion rate approaches the critical value $\dot{m}_{\rm cr}$ corresponding to the Eddington luminosity, the standard model becomes inconsistent. Inside some radius r_t, the produced radiation is trapped by the flow and advected into the black hole, as the inflow time-scale here is less than the time-scale of photon escape from the disk, $\sim \tau H/c$, (Begelman & Meier 1982). The trapping radius can be estimated from the standard model of Shakura & Sunyaev (1973) by comparing the radial flux of internal energy $3c_s^2\dot{M}$ with the total flux of radiation emitted outside r. One then gets $r_t \approx 7r_g$ for $\dot{m}=\dot{m}_{\rm cr}=12$. The relative height of the standard disk, H/r, equals $\dot{m}/27$ at the maximum. Advection thus starts to become important before the accretion flow becomes quasi-spherical, and it may be approximately treated retaining the vertically-integrated approximation.

Advection reduces the vertical radiation flux F^- as compared to the standard model and, as a result, the disk thickness stays moderate at super-critical accretion rates (Abramowicz et al. 1988; Chen & Taam 1993). This made possible an extension of the 1D model to the super-Eddington advection dominated regime, called "slim" accretion disk. The slim model may apply at moderately super-critical accretion rates. In the limit $\dot{m} \gg \dot{m}_{\rm cr}$ there appears an extended region where the accretion flow has a positive Bernoulli constant, and the bulk of supplied gas may be pushed away by the radiation pressure to form a wind (Shakura & Sunyaev 1973). The behavior of the flow at $\dot{m} \gg \dot{m}_{\rm cr}$ still remains an open issue. Detailed 2D hydrodynamical simulations might clarify whether gas mainly falls into the black hole or flows out (Eggum, Coroniti & Katz 1988; Igumenshchev & Abramowicz 1998).

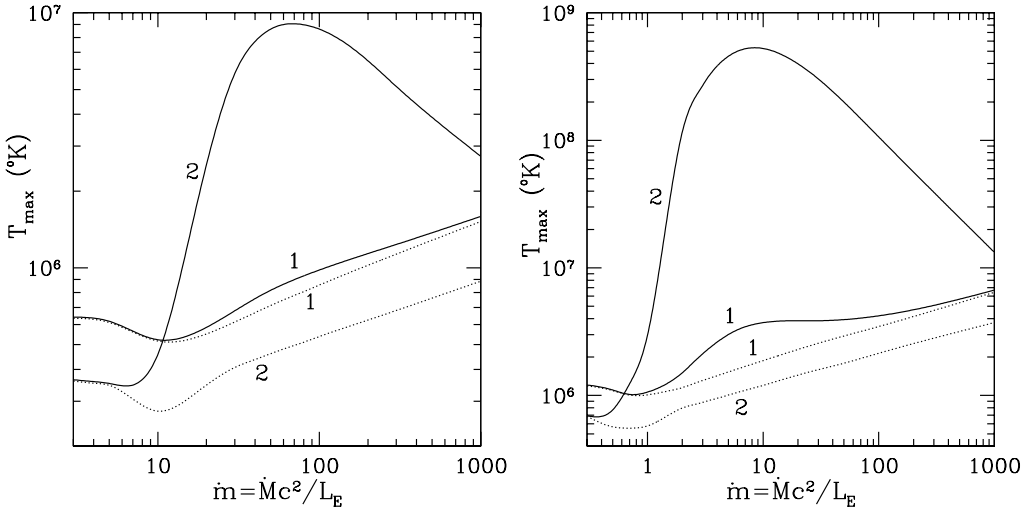

Figure 1. The temperature in the innermost region of the disk versus $\dot{m}$ for Schwarzschild ($a_* = 0$, $\dot{m}_{\rm cr} = 17.5$, *left panel*) and Kerr ($a_* = 0.998$, $\dot{m}_{\rm cr} = 3.11$, *right panel*) black holes in the cases of $\alpha = 0.03$ (marked 1) and $\alpha = 0.3$ (marked 2). A black hole mass $M = 10^8 M_\odot$ is assumed. The dotted curves show the blackbody temperature $T_{\rm eff}$. (From Beloborodov 1998a.)

The relativistic slim disk has been calculated in Beloborodov (1998a) for both non-rotating ($a_* = 0$) and rapidly rotating ($a_* = 0.998$) black holes. Like its pseudo-Newtonian counterpart, the relativistic slim disk has a moderate height up to $\dot{m} \sim 10\dot{m}_{\rm cr}$ due to advection of the trapped radiation. An important issue is the temperature of the accreting gas as the temperature determines the emission spectrum. The simplest way to evaluate the temperature is by assuming that the gas is in thermodynamic equilibrium with the radiation density in the disk, w. Then T equals $T_{\rm eff} = (w/a_r)^{1/4}$ where, a_r is the radiation constant. This was usually adopted in models of super-critical disks. The blackbody approximation, however, fails when $\alpha > 0.03$ (Beloborodov 1998a). The gas then accretes so fast and has so low density that it is unable to reprocess the released energy into Planckian radiation. As a result, gas overheats so that $T \gg T_{\rm eff}$.

The possibility of the overheating in near-critical disks was pointed out by Shakura & Sunyaev (1973) and discussed later (e.g., Liang & Wandel 1991; Björnsson et al. 1996). In the standard model, the disk density scales as $n \propto \dot{m}^{-2}$, while the heating rate $F^+ \propto \dot{m}$. The resulting temperature of the overheated gas increases with $\dot{m}$. The slim disk model allows one to follow this tendency toward the super-critical regime. Figure 1 shows the results for a massive black hole in an AGN. The strongest overheating occurs at $\dot{m} \sim 3 - 4\ \dot{m}_{\rm cr}$. At $\dot{m} \gg \dot{m}_{\rm cr}$ the density increases, $n \propto \dot{m}$, and the temperature falls down. A similar overheating occurs in GBHs ($M \sim 10 M_\odot$) if $\alpha > 0.1$.

The main process cooling the plasma in overheated disks with large $\dot{M}$ is the saturated Comptonization of bremsstrahlung photons (cf. Rybicki & Lightman 1979). The plasma temperature is determined by the heating=cooling balance

(Beloborodov 1998a),

$$\dot{w}^+ \equiv \frac{F^+}{2H} \approx \dot{w}_{\rm ff} \left[\frac{w}{w_{\rm pl}} + A \left(1 - \frac{w}{w_{\rm pl}} \right) \right] \left(1 - \frac{w}{w_{\rm pl}} \right), \qquad (9)$$

where $\dot{w}_{\rm ff} = 1.6 \cdot 10^{-27} n^2 \sqrt{T}$ is the free-free cooling rate, $w_{\rm pl} = a_r T^4$, and A is the Compton amplification factor. In the optically thick limit ($w_{\rm pl} \approx w$) this equation yields $\dot{w}^+ = \dot{w}_{\rm ff}(1 - w/w_{\rm pl})$, while in the overheated case ($w_{\rm pl} \gg w$) it transforms into $\dot{w}^+ = A\dot{w}_{\rm ff}$. The Compton amplification factor achieves $A \sim 300$ in the hottest models. The efficient Compton cooling prevents a transition to an extremely hot two-temperature state (see also Björnsson et al. 1996).

The overheating will strongly affect the disk spectrum: the spectrum of a relativistic disk with $\dot{m} \gtrsim \dot{m}_{\rm cr}$ can extend to the hard X-ray band, in contrast to the spectra of blackbody pseudo-Newtonian models (Szuszkiewicz, Malkan & Abramowicz 1996).

Many GBHs and AGNs, however, accrete at sub-Eddington rates and their hard X-ray emission implies a different mechanism.

5. Two-temperature disks

5.1. The SLE model

To explain the hard spectrum of the classical black hole candidate Cyg X-1, Shapiro, Lightman & Eardley (1976, hereafter SLE) suggested a two-temperature model of an accretion disk with protons much hotter than electrons, $T_p \gg T_e$. The hot proton component then dominates the pressure and keeps the disk geometrically thick. This in turn leads to a low density which scales $\propto H^{-3}$ for given $\dot{m}$ and α. A low density implies a low rate of Coulomb energy exchange between the protons and the electrons and allows one to keep $T_p \gg T_e$ self-consistently.

The four main equations of the disk structure are the same as in the standard model (see Section 2). The SLE disk has two temperatures. Therefore, the heating=cooling balance is now described by two equations:

i) Energy balance for the protons. The model assumes that viscous dissipation heats preferentially the protons and then the bulk of this energy is transferred to the electrons through Coulomb collisions, i.e.,

$$\frac{F^+}{2H} = \frac{nkT_p}{t_{ep}}, \qquad \text{where} \qquad t_{ep} \approx 17 \frac{T_e^{3/2}}{n}$$

is the Coulomb cooling time (with a Coulomb logarithm ≈ 15, see Spitzer 1962). This equation yields

$$\theta_p \theta_e \approx 10^{-2} \frac{\dot{m}^{2/3}}{\alpha^{4/3}} \left(\frac{r}{r_g} \right)^{-1} S^{-2/3}, \qquad (10)$$

where $\theta_e \equiv kT_e/m_e c^2$ and $\theta_p \equiv kT_p/m_p c^2$.

ii) Energy balance for the electrons. The electrons cool mainly by upscattering soft radiation coming from an outer cold disk or from dense cloudlets

embedded in the hot flow. The cooling proceeds in the regime of unsaturated Comptonization (cf. SLE). In this regime, the disk parameters adjust so that $y = 4\theta_e \max(\tau, \tau^2) \approx 1$. Typically, $\theta_e \lesssim 1$ and $\tau \sim 1$. The condition $y \approx 1$ gives

$$\frac{\theta_p}{\theta_e} \approx \frac{\sqrt{2}\dot{m}}{\alpha}\left(\frac{r}{r_g}\right)^{-3/2} \text{ if } \tau \lesssim 1 \qquad \text{and} \qquad \frac{\theta_p^2}{\theta_e} \approx \frac{\dot{m}^2}{2\alpha^2}\left(\frac{r}{r_g}\right)^{-3} \text{ if } \tau > 1. \quad (11)$$

Equations (10-11) yield an electron temperature that weakly depends on radius, $\theta_e \approx 0.1(\alpha\dot{m})^{-1/6}(r/r_g)^{1/4}$. The complete set of equations allows one to express the other disk parameters as functions of radius (see SLE). In particular, the proton temperature and the disk height are $(H/r)^2 \sim \theta_p/\theta_{\rm vir} \sim 0.1\alpha^{-4/3}\dot{m}^{2/3}(r/r_g)^{-1/4}$ where $\theta_{\rm vir} \sim r_g/r$ is the virial temperature.

The model was further developed to include effects of pair production (e.g., Liang 1979b; Björnsson & Svensson 1992; Kusunose & Mineshige 1992), a non-thermal particle distribution (Kusunose & Mineshige 1995), and cyclosynchrotron radiation (Kusunose & Zdziarski 1994). A relativistic version of the SLE disk around a Kerr black hole was calculated by Björnsson (1995).

The SLE model is in agreement with observed spectra of GBHs and AGNs. The shortcoming of the model is that it is thermally unstable (Pringle 1976; Piran 1978): the assumed energy balance would be destroyed by a small perturbation of the proton temperature. An increase in T_p would result in disk expansion in the vertical direction. Then the Coulomb cooling is reduced (and the heating rate is increased) and T_p increases further, leading to an instability.

5.2. The ADAF model

In the SLE model only a fraction of the dissipated energy remains in the proton component to keep it hot, and the bulk of the energy is passed to the electrons and radiated. Ichimaru (1977) considered a disk of so low density that the heated protons are unable to pass their energy to the electrons on the time-scale of accretion. The protons then accumulate the energy and advect it. Such a flow is thermally stable. It emits only a fraction of the dissipated energy that has been passed directly to the electrons.

If viscous dissipation heats mostly the protons, then the radiative efficiency of the accretion flow is very low, and the energy is either advected into the black hole (Ichimaru 1977; Rees et al. 1982) or transported outward in the form of a hot wind (Blandford & Begelman 1998, see also Begelman, these proceedings). The former case (ADAF) may be modeled in 1D approximation (see Narayan et al. 1998 for a review). The latter case requires detailed 2D simulations (Igumenshchev & Abramowicz 1998) which are much more difficult: the very formulation of a 2D problem implies additional assumptions (local viscosity prescription, local heating rate, and 2D boundary conditions).

The assumption that protons are heated preferentially has recently been assessed (see Quataert & Gruzinov 1998; Quataert, these proceedings, and references therein). It was argued that the dissipation of Alfvénic turbulence in the disk may heat mostly protons only if the magnetic energy density is $\lesssim 10\%$ of the proton pressure. If the magnetic field is the source of viscosity, one expects $\alpha < 0.1$ in a two-temperature disk.

The necessary condition for ADAF models is that the time-scale for Coulomb cooling, t_{ep}, exceeds the accretion time-scale, $t_a \approx (\alpha\Omega_{\rm K})^{-1}$. It requires

$$\dot{m} \lesssim 10^2 \alpha^2 \theta_e^{3/2}.$$

The typical electron temperature in the calculated ADAF models is $\sim 10^9$ K (e.g., Nakamura et al. 1997; Esin et al. 1998), and the corresponding maximum accretion rate is

$$\dot{m}_{\rm max} \sim 10\alpha^2. \tag{12}$$

From hydrodynamical point of view, the two-temperature ADAFs are similar to the super-critical disks. Again, most of the dissipated energy is stored inside the disk and it swells up to a quasi-spherical shape. The radial pressure gradients and deviations from Keplerian rotation are dynamically important, and the full set of differential equations should be solved to obtain a solution for the disk structure (Chen, Abramowicz & Lasota 1997; Narayan, Kato & Honma 1997). At large distances, $r \gg r_g$, the ADAF parameters have a power-law dependence on radius (Narayan & Yi 1994). An approximate description of the advective disk was given by Abramowicz et al. (1995) who assumed that the disk rotates with a Keplerian velocity in the pseudo-Newtonian potential. Recently, relativistic solutions have been calculated for ADAFs in Kerr geometry (Abramowicz et al. 1996; Peitz & Appl 1997; Igumenshchev, Abramowicz & Novikov 1998; Popham & Gammie 1998) and the expected spectra have been discussed (Jaroszyński & Kurpiewski 1997). The ADAF model is applied mainly to low luminosity objects with suspected black holes, such as Sgr A*, nuclei of elliptical galaxies, and X-ray novae in quiescent state (see Narayan et al. 1998 and references therein).

The possibility of a two-temperature accretion flow in Cyg X-1 and other GBHs in the hard state has again been addressed by Narayan (1996), Esin et al. (1998), and Zdziarski (1998). Their basic picture of accretion is the same as in the SLE model: at some radius $r_{\rm tr}$, the standard "cold" disk undergoes a transition to a hot two-temperature flow which emits hard X-rays by Comptonizing soft radiation in the unsaturated regime. In contrast to SLE, radial advection of heat is taken into account, and the parameters ($\dot{m}$ and α) are chosen so that advection and radiative cooling are comparable. Then the flow is a good emitter and at the same time it may be stabilized by advection. It implies that the accretion rate is just at the upper limit (eq. [12]), and $\alpha \sim 0.3$ has to be assumed, as typically $\dot{m} \sim 1$ in GBHs. The optical depth of the flow near the black hole is approximately

$$\tau \sim \frac{\dot{m}}{\alpha} \sim 1.$$

Combined with the typical electron temperature $T_e \sim 10^9$ K, this yields $y \sim 1$, just what is needed to be in the regime of unsaturated Comptonization that is believed to generate the X-ray spectrum.

An advantage of a hot disk model is its consistency with the observed weak X-ray reflection in GBHs in the hard state (Ebisawa et al. 1996; Gierliński et al. 1997; Zdziarski et al. 1998; Życki, Done & Smith 1998). Observations suggest that cold gas reflecting the X-rays covers a modest solid angle $\Omega \sim 0.3 \times 2\pi$ as viewed from the X-ray source. This is consistent with the outer cold + inner

hot flow geometry (for alternative models see Section 6.4). Provided the two conditions $\dot{m} \approx \dot{m}_{\rm max}$ and $\tau \sim 1$ are satisfied, and the inner radius of the cold disk, $r_{\rm tr}$, is properly chosen, the advective model may approximately describe the hard state of GBHs. A small increase ($\sim$ 10 %) in $\dot{m}$ would then result in a transition to the soft state, as the hot flow collapses to a standard thin disk (Esin et al. 1998). A similar small decrease in $\dot{m}$ would lead to transition to a low-efficiency ADAF which may be associated with the quiescent state in transient sources.

There is then a question, why the hard state is so widespread if it requires the fine-tuning of both $\dot{m}$ and α? In particular, why the hard state is stable in Cyg X-1 while its luminosity varies by a factor of ~ 2? Variations in luminosity are presumably due to variations in $\dot{m}$ and, according to the ADAF model, the change in $\dot{m}$ must switch off the hard state and cause a transition to the soft or quiescent state. The latter has never been observed in Cyg X-1. Moreover, the observed slope of the X-ray spectrum in the hard state is kept constant with varying luminosity (Gierliński et al. 1997), which indicates a persistent y-parameter of the emitting plasma.

One possible explanation is that the disk has $\dot{m} > \dot{m}_{\rm max}$, being composed of two phases, hot and cold. The thermal instability of a hot disk at $\dot{m} > \dot{m}_{\rm max}$ may continue to produce a cold phase until $\dot{m}$ in the hot phase is reduced to $\dot{m}_{\rm max}$. Then a balance between the cold and hot phases might keep both conditions $\dot{m} \approx \dot{m}_{\rm max}$ and $\tau \sim 1$ for the hot phase (Zdziarski 1998). Hot accretion disks with cold clumps of gas have recently been discussed in different contexts (Kuncic, Celotti & Rees 1997; Celotti & Rees, these proceedings; Krolik 1998; Krolik, these proceedings). The cold clumps may also play a role as a source of seed soft photons for Comptonization (e.g., Zdziarski et al. 1998).

The dynamics of a cold phase produced in the hot disk is, however, a very complicated and unresolved issue. In particular, it is unclear whether the cold phase may accrete independently with its own radial velocity, or if it rather is "frozen" in the hot phase. The cold clumps moving through the hot medium should be violently unstable, and a model for dynamical equilibrium is needed for a continuously disrupted/renewed cold phase. If the clump life-time exceeds the time-scale for momentum exchange with other clumps and/or with the hot medium, then the clumps should settle down to the equatorial plane and form a cold thin disk. One then arrives at the disk-corona model.

6. The disk-corona model

6.1. Magnetic flares

That the observed X-rays can be produced in a hot corona of a relatively cold accretion disk extending all the way to the black hole was suggested a long time ago (e.g., Bisnovatyi-Kogan & Blinnikov 1977; Liang 1979a). Most likely, a low density corona is heated by reconnecting magnetic loops emerging from the disk (Galeev, Rosner & Vaiana 1979, hereafter GRV). This implies that the corona is coupled to the disk by the magnetic field (for alternative models, where the corona accretes fast above the disk, see, e.g., Esin et al. 1998; Witt, Czerny & Życki 1997; Czerny et al., these proceedings).

The usually exploited model for the corona formation is that of GRV. According to the model, a seed magnetic field is exponentially amplified in the disk due to a combination of the differential Keplerian rotation and the turbulent convective motions. The amplification time-scale at a radius r is given by $t_{\rm G} \sim r/3v_c$ where v_c is a convective velocity. GRV showed that inside luminous disks the field is not able to dissipate at the rate of amplification. Then buoyant magnetic loops elevate to the corona where the Alfvénic velocity is high and the magnetic field may dissipate quickly.

The coronal heating by the GRV mechanism is, however, not sufficient to explain the hard state of GBHs (Beloborodov 1999). The rate of magnetic energy production per unit area of the disk equals $F_B = 2H\overline{w}_B/t_{\rm G}$ where $\overline{w}_B = \overline{B^2}/8\pi$ is the average magnetic energy density in the disk at a radius r. One can compare F_B with the total dissipation rate, $F^+ = 3t_{r\varphi}c_{\rm s}$, to get

$$\frac{F_B}{F^+} = \frac{H}{r}\frac{t^B_{r\varphi}}{t_{r\varphi}}.$$

Here $t^B_{r\varphi} = \overline{B_\varphi B_r}/4\pi$ and we took into account that $B_\varphi/B_r = c_{\rm s}/v_{\rm c}$ in the GRV model. Hence, the GRV mechanism is able to dissipate only a small fraction $\sim H/r \ll 1$ of the total energy released in the disk.

Recent simulations of MHD turbulence indicate that the magneto-rotational instability efficiently generates magnetic energy in the disk (see Balbus & Hawley 1998). The instability operates on a Keplerian time-scale, which is $\sim H/r$ times shorter than $t_{\rm G}$, and it produces magnetic energy at a rate $F_B \sim F^+$. A low dissipation rate inside the disk would lead to buoyant transport of generated magnetic loops to the corona (GRV). The hard state of an accretion disk may be explained as being due to such a "corona-dominated" dissipation. By contrast, in the soft state, the bulk of the energy is released inside the optically thick disk and the coronal activity is suppressed.

In the hard state, the corona is the place to which magnetic stress driving accretion is transported and released. Conservation of angular momentum reads (see eq.[4])

$$2Ht_{r\varphi} = \frac{\dot{M}}{2\pi}\Omega_{\rm K}S.$$

For a standard radiation-pressure-dominated disk it gives $t_{r\varphi} \approx m_p c\Omega_{\rm K}/\sigma_{\rm T}$. If a large fraction, ζ, of F^+ is dissipated above the cold disk, then the disk height is reduced by a factor $(1-\zeta)$ (Svensson & Zdziarski 1994). It implies that $t_{r\varphi}$ is increased by a factor $(1-\zeta)^{-1}$. The magnetic corona is expected to be inhomogeneous and the main dissipation probably occurs in localized blobs where the magnetic energy density w_B is much larger than the average $t_{r\varphi}$. The accumulated magnetic stress in such a blob may suddenly be released on a time-scale $t_0 \sim 10r_b/c$ (the "discharge" time-scale, see Haardt, Maraschi & Ghisellini 1994) where r_b is the blob size. This produces a compact flare of luminosity $L \sim r_b^3 w_B/t_0$.

In this picture of the hard state, the binding energy of spiraling gas is liberated in intense flares atop the accretion disk. There is no detailed model for the magnetic flare phenomenon despite the fact that magnetic flares have been studied for many years in the context of solar activity. In particular, it is unclear

whether the flaring plasma should be thermal or non-thermal. Observations therefore play a crucial role in developing a model. Observed X-ray spectra of black hole sources suggest that the bulk of emission comes from a thermal plasma with a typical temperature $kT \sim 50 - 200$ keV and Thomson optical depth $\tau_{\rm T} \sim 0.5 - 2$ (see Zdziarski et al. 1997; Poutanen 1998). The narrow dispersion of the inferred T and $\tau_{\rm T}$ indicates the presence of a standard emission mechanism.

One possible scenario has been developed assuming a large compactness parameter of the flares $l = L\sigma_{\rm T}/r_b m_e c^3 \sim 10 - 10^3$. Then the flare gets dominated by $e^{\pm}$ pairs created in $\gamma - \gamma$ interactions (e.g., Svensson 1986). The pairs produced tend to keep $\tau_{\rm T} \sim 0.5 - 2$ and $kT \sim 50 - 200$ keV, in excellent agreement with observations. Yet, it is also possible that the flares are dominated by a normal proton plasma with $\tau_{\rm T} \sim 1$. Improved data should help to distinguish between the models. In particular, detection of an annihilation feature in the X-ray spectra would help.

6.2. Compton cooling

A flaring blob cools mainly by upscattering soft photons. We will hereafter assume that soft radiation comes from the underlying disk of a temperature T_s. The additional source of seed soft photons due to the cyclo-synchrotron emission in the blob is discussed, e.g., by Di Matteo, Celotti & Fabian (1997) and Wardziński & Zdziarski (these proceedings). When a soft photon of initial energy ε_s passes through the flare, it acquires *on average* an energy $A\varepsilon_s$, where A is the Compton amplification factor. A may also be expressed as $A = (L_{\rm diss} + L_s)/L_s$ where $L_{\rm diss}$ is the power dissipated in the flare and L_s is the intercepted soft luminosity.

The produced X-rays have a power-law spectrum whose slope Γ depends on the relativistic y-parameter of the blob, $y = 4(\theta_e + 4\theta_e^2)\tau_{\rm T}(\tau_{\rm T} + 1)$. Leaving aside the effects of the (unknown) geometry of the blob, one may evaluate Γ by modeling radiative transfer in the simplest one-zone approximation in terms of an escape probability, as done, e.g., in the code of Coppi (1992). We have calculated the photon spectral index Γ using Coppi's code (see Figure 2). Within a few percent Γ follows a power law

$$\Gamma \approx \frac{9}{4} y^{-2/9}. \tag{13}$$

This empirical relation is simpler than the approximation of Pozdnyakov, Sobol & Sunyaev (1979), $\Gamma \approx 1 + [2/(\theta_e + 3) - \log \tau_{\rm T}]/\log(12\theta_e^2 + 25\theta_e)$.

One may also evaluate Γ as a function of the Compton amplification factor. Then the result depends on T_s which is typically a few $\times 10^6$ K in GBHs and a few $\times 10^4$ K in AGNs. The corresponding dependences $\Gamma(A)$ are shown in Figure 2b. To high accuracy ($\sim 3 - 4$ %), the results can be approximated as

$$\Gamma \approx \frac{7}{3}(A - 1)^{-\delta}, \tag{14}$$

where $\delta \approx 1/6$ for GBHs and $\delta \approx 1/10$ for AGNs. Formula (14) is more accurate than the estimate of Pietrini & Krolik (1995), $\Gamma \approx 1 + 1.6(A-1)^{-1/4}$, where the dependence on T_s is neglected.

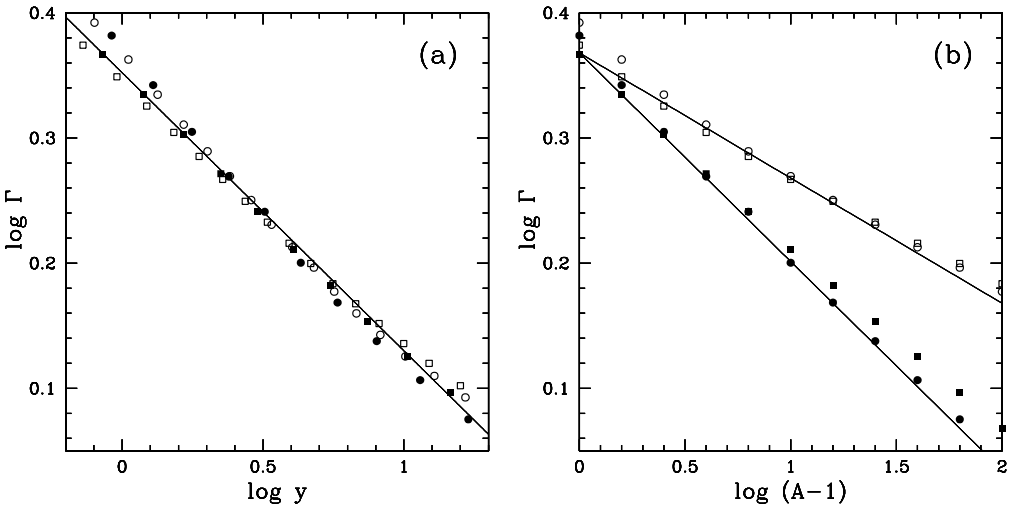

Figure 2. (a) X-ray spectral index, Γ, versus y-parameter. Open circles – $kT_s = 5$ eV, $kT = 50$ keV, open squares – $kT_s = 5$ eV, $kT = 100$ keV, filled circles – $kT_s = 200$ eV, $kT = 50$ keV, filled squares – $kT_s = 200$ eV, $kT = 100$ keV. The line shows the approximation (13). (b) Γ versus $A - 1 = L_{\rm diss}/L_s$. The two lines show the approximation (14) with $\delta = 1/10$ and $\delta = 1/6$.

6.3. The feedback of X-ray reprocessing by the disk

The flares illuminate the underlying accretion disk that must reflect/reprocess the incident X-rays. The disk produces important features in the observed X-ray spectrum, such as the Fe Kα line and the Compton reflection bump, as extensively discussed in these proceedings. Even more important, the disk reprocesses a significant part of the X-ray luminosity into soft radiation. As the flare is expected to dominate the local disk emission, the reprocessed radiation becomes the main source of soft photons. Then the flares are "self-regulating": the flare temperature adjusts to keep $A = (L_s/L)^{-1}$ where L_s/L is a fraction of the flare luminosity that comes back as reprocessed radiation (Haardt & Maraschi 1993; Haardt et al. 1994). The resulting spectral slope is determined by the feedback of reprocessing, L_s/L. Detailed calculations of the predicted X-ray spectrum were performed by Stern et al. (1995) and Poutanen & Svensson (1996) and applied to Seyfert 1 AGNs (see Svensson 1996 for a review).

The calculated models are, however, in conflict with observations of Cyg X-1 and similar black hole sources in the hard state (e.g., Gierliński et al. 1997): i) The observed hard spectrum corresponds to a Compton amplification factor $A \gtrsim 10$ and implies soft photon starvation of the hot plasma, $L_s \ll L$. The model predicts $A \lesssim 5$ unless the active blobs are elevated above the disk at heights larger than the blob size (Svensson 1996). ii) The model with elevated blobs would yield a strong reflection component, $R = \Omega/2\pi \approx 1$, where Ω is the solid angle covered by the cold matter as viewed from the X-ray source. The reported amount of reflection is small, $R \sim 0.3$.

The weak reflection and soft photon starvation may be explained if the cold reflector is disrupted near the black hole. This would agree with the idea that accretion proceeds as a hot two-temperature flow in the inner region as discussed in Section 5. One may fit observed spectra with a toy model of a hot central cloud upscattering soft photons supplied by a surrounding cold disk or by dense clumps inside the hot region (e.g., Poutanen, Krolik & Ryde 1997; Zdziarski et al. 1998). The transient soft state is then explained as being due to shrinking of the hot region, so that the cold disk extends all the way to the black hole and the bulk of the energy is dissipated inside the optically thick material of the disk (Poutanen et al. 1997; Esin et al. 1998).

However, the weak reflection does not necessarily imply that the inner cold disk is disrupted in the hard state. One suggested alternative is that the apparent weakness of the reflection features is due to a high ionization of the upper layers of the disk (Ross, Fabian & Young 1998). Another alternative is that the emitting hot plasma has a bulk velocity directed away from the disk (Beloborodov 1999). Mildly relativistic bulk motion causes aberration reducing X-ray emission towards the disk. It in turn reduces the feedback of reprocessing and leads to a hard X-ray spectrum.

The coupling between the flare and the underlying disk can be approximately described assuming that the luminosity emitted downwards within an angle $\cos^{-1}\mu_s$ comes back to the flare. The effective μ_s depends on the flare geometry. E.g., a slab geometry of the active region corresponds to $\mu_{\rm s}=0$, and an active hemisphere atop the disk has $\mu_{\rm s}\approx 0.5$. The feedback factor, L_s/L, of a flare of luminosity L atop the disk is determined by three parameters:

- The geometrical parameter $\mu_{\rm s}$.
- The bulk velocity in the flare, $\beta=v/c$ (assumed to be perpendicular to the disk).
- The disk albedo, a. $\chi=1-a$ represents the efficiency of reprocessing of the incident X-rays.

In the static case ($\beta=0$), the reflection $R=1$ and $L_s=L\chi(1-\mu_{\rm s})/2$. The corresponding amplification factor is $A=2/\chi(1-\mu_{\rm s})$. With increasing β, A increases, and R is reduced. The impact of a bulk velocity on A and R is summarized in Figure 3a for several $\mu_{\rm s}$ and system inclinations θ. In the calculations, we assumed a typical albedo $a=0.15$ (e.g., Magdziarz & Zdziarski 1995). Note that the observed R may be further reduced because the reflected radiation is partly upscattered by the blob.

One can evaluate the spectral index of a flare using equation (14). For a typical $\mu_{\rm s}\sim 0.5$ one gets $\Gamma\approx 1.9B^{-0.5}$ for GBHs and $\Gamma\approx 2B^{-0.3}$ for AGNs, where $B\equiv\gamma(1+\beta)$ is the aberration factor due to bulk motion (Beloborodov 1999). E.g., for Cyg X-1 in the hard state, both the spectral slope $\Gamma\sim 1.6$ and the amount of reflection $R\sim 0.3$ can be explained assuming $\beta\sim 0.3$.

6.4. The ejection model

The inferred $\beta>0$ implies that the flares are accompanied by plasma ejection from the active regions, in contrast to the static corona model. In fact, one

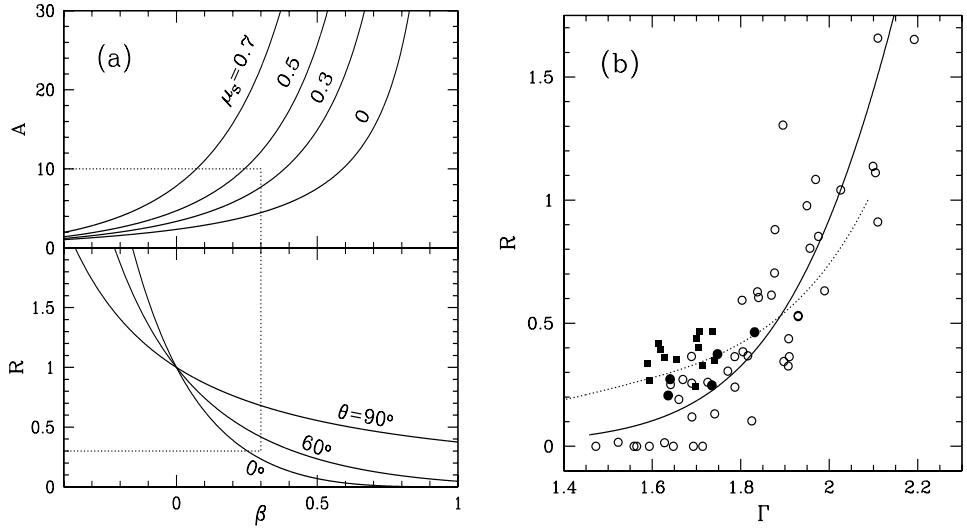

Figure 3. (a) *Top:* Compton amplification, A, of the reprocessed radiation as a function of β. A disk albedo $a = 0.15$ is assumed. *Bottom:* Apparent amount of reflection, R. The dotted line shows expected A and R for $\beta = 0.3$. (From Beloborodov 1999.)
(b) Best fits to Γ and R for a number of AGNs (open circles), Cyg X-1 (filled squares), and GX 339-4 (filled circles). The data are from Zdziarski et al. (1999). The solid curve shows the correlation $R(\Gamma)$ predicted by the ejection model for AGNs (assuming $\mu_{\rm s} = 0.55$ and inclination $\theta = 45^{\rm o}$). $R(\Gamma)$ predicted for AGNs by the hot disk model (see Zdziarski et al. 1999) is shown by the dotted line.

should expect bulk motion of a flaring plasma on theoretical side, especially if the plasma is composed of light $e^{\pm}$ pairs. There is at least one reason for bulk acceleration: the flare luminosity, L, is partly reflected from the disk, and hence the flaring plasma is immersed in an anisotropic radiation field. The net radiation flux, $\sim L/r_b^2$, is directed away from the disk and it must accelerate the plasma. The transferred momentum per particle per light-crossing time, r_b/c, is $\sim lm_ec$ where $l = L\sigma_{\rm T}/r_bm_ec^3$ is the compactness parameter of the flare. Hence, the acceleration time-scale is $t_a \sim l^{-1}r_b/c$ for a pair plasma and $t_a \sim (m_p/m_e)l^{-1}r_b/c$ for a normal proton plasma. The shortness of t_a for a pair plasma implies that the pair bulk velocity saturates at some equilibrium value limited by the radiation drag. Using a simple toy model, one may estimate the expected velocity to be in the range $\beta \sim 0.1-0.7$ (Beloborodov 1999). A proton plasma may also be accelerated to relativistic velocities if the flare duration exceeds t_a, which is quite probable.

The very magnetic dissipation may be accompanied by pumping a net momentum into the flare at a rate $\sim L/c$. When the stored magnetic energy gets released, the heated plasma may be ejected both toward and away from the disk. Again, the large compactness parameter implies efficient momentum transfer to the plasma, $\sim lm_ec$ per particle per light crossing time. Possible ejection toward the disk corresponds to $\beta < 0$.

Plasma ejection from magnetic flares is likely to occur in both GBHs and AGNs. The plasma velocity may vary. An increase in β leads to decreasing R and Γ. A correlation between R and Γ is observed in GBHs and AGNs (Zdziarski, Lubiński & Smith 1999; Zdziarski, these proceedings) and it is well reproduced by the ejection model, see Figure 3b. The theoretical curve is plotted for AGNs, assuming a disk albedo $a = 0.15$, $\mu_s = 0.55$, and inclination $\theta = 45^{\rm o}$. These parameters are probably the most representative. The dispersion of data around the curve might be due to a dispersion in $\mu_{\rm s}$ and inclination angles. The velocity, β, varies from -0.2 to 0.75; $R = 1$ corresponds to $\beta = 0$.

The two model curves shown in Figure 3b are calculated for AGNs ($\delta = 1/10$ in eq. [14]). For GBHs, Γ should be systematically smaller as a result of a higher energy of seed soft photons. This tendency is seen in Figure 3b: the Cyg X-1 and GX 339-4 data are shifted to the left as compared to the AGN data.

Outflows are usually expected in radio-loud objects where they have been considered as a possible reason for weak Compton reflection (Woźniak et al. 1998). Figure 3b may indicate that plasma acceleration in X-ray coronas of accretion disks is a common phenomenon in black hole sources. Note also that fast outflows may manifest themselves in optical polarimetric observations of AGNs (Beloborodov 1998b; Beloborodov & Poutanen, these proceedings).

7. Concluding remarks

Disk-like accretion may proceed in various regimes. Any specific model is based on assumptions including prescriptions for the effective viscosity, the vertical distribution of the ion/electron heating, the energy transport out of the disk, etc. Large uncertainties in these prescriptions allow one to produce a lot of models, and observations should help to choose between them. Hard X-ray observations play an important role in this respect. They indicate that a large fraction of the accretion energy is released in a rarefied plasma (corona) where the X-rays are generated by unsaturated Comptonization of soft photons. In most cases, the accreting mass is expected to be concentrated in a "cold" phase, probably forming a thin disk embedded in the corona. Its gravitational energy transforms into the magnetic energy that is subsequently released in the corona.

Most likely, the dissipation mechanism is related to highly non-linear MHD which usually produces inhomogeneous and variable dynamical systems. In particular, the energy release in the corona is likely to proceed in magnetic flares generating observed temporal and spectral X-ray variability. Idealized hydrodynamical models are unable to describe this process. The difficulty of the problem is illustrated by the activity of the Sun, where theoretical progress is modest despite the fact that detailed observations are available. In accretion disks, magnetic fields are likely to play a crucial dynamical role and various plasma instabilities may take place. The instabilities probably govern the distribution of the plasma density and the heating rate.

Given the difficulty of the accretion physics, studies of phenomena having specific, observationally testable implications, are especially useful. In particular, the reflection and reprocessing of the corona emission by the cold disk provides diagnostics for accretion models. We here discussed a plausible phenomenon – bulk acceleration of the flaring plasma in the corona – that strongly

affects the reflection pattern and the radiative coupling between the corona and the cold disk.

Acknowledgments. I thank J. Poutanen, R. Svensson, and A. A. Zdziarski for discussions and comments on the manuscript. I am grateful to Andrzej Zdziarski for providing the $R - \Gamma$ correlation data prior to publication and to Paolo Coppi for his EQPAIR code. This work was supported by the Swedish Natural Science Research Council and RFFI grant 97-02-16975.

References

Abramowicz, M. A., Chen, X., Granath, M., & Lasota, J.-P. 1996, ApJ, 471, 762

Abramowicz, M. A., Chen, X., Kato, S., Lasota, J.-P., & Regev, O. 1995, ApJ, 438, L37

Abramowicz, M. A., Czerny, B., Lasota, J.-P., & Szuszkiewicz, E. 1988, ApJ, 332, 646

Abramowicz, M. A., Lanza, A., & Percival, M.J. 1997, ApJ, 479, 179

Artemova, I. V., Björnsson, G., & Novikov, I. D. 1996, ApJ, 461, 565

Balbus, S. A., & Hawley, J. F. 1998, Rev. Mod. Phys., 70, 1

Begelman, M. C., & Meyer, D. L. 1982, ApJ, 253, 873

Beloborodov, A. M. 1998a, MNRAS, 297, 739

Beloborodov, A. M. 1998b, ApJ, 496, L105

Beloborodov, A. M. 1999, ApJ, 510, L123

Beloborodov, A. M., Abramowicz, M. A., & Novikov, I. D. 1997, ApJ, 491, 267

Blandford, R. D., & Begelman, M. C. 1998, MNRAS, in press

Bisnovatyi-Kogan, G. S., & Blinnikov, S. I. 1977, A&A, 59, 111

Björnsson, G., Abramowicz, M. A., Chen, X., & Lasota, J.-P. 1996, ApJ, 467, 99

Björnsson, G. 1995, ApJ, 441, 765

Björnsson, G., & Svensson, R. 1992, ApJ, 394, 500

Chen, X., Abramowicz, M. A., & Lasota, J.-P. 1997, ApJ, 476, 61

Chen, X., & Taam, R. E. 1993, ApJ, 412, 254

Coppi, P. S. 1992, MNRAS, 258, 657

Di Matteo, T., Celotti, A., & Fabian, A. C. 1997, MNRAS, 291, 805

Ebisawa, K., Ueda, Y., Inoue, H., Tanaka, Y., & White, N. E. 1996, ApJ, 467, 419

Eggum, G. E., Coroniti, F. V., & Katz, J. I. 1988, ApJ, 330, 142

Esin, A. A., Narayan, R., Cui, W., Grove, J. E., & Zhang, S.-N. 1998, ApJ, 505, 854

Galeev, A. A., Rosner, R., & Vaiana, G. S. 1979, ApJ, 229, 318

Ghisellini, G., Guilbert, P. W., & Svensson, R. 1988, ApJ, 334, L5

Gierliński, M., Zdziarski, A. A., Done, C., Johnson, W. N., Ebisawa, K., Ueda, Y., Haardt, F., & Phlips, B. F. 1997, MNRAS, 288, 958

Haardt, F., & Maraschi, L. 1993, ApJ, 413, 507

Haardt, F., Maraschi, L., & Ghisellini, G. 1994, ApJ, 432, L95

Ichimaru, S. 1977, ApJ, 214, 840

Igumenshchev, I. V., & Abramowicz, M. A. 1998, MNRAS, in press

Igumenshchev, I. V., Abramowicz, M. A., & Novikov, I.D. 1998, MNRAS, 298, 1069

Jaroszyński, M., & Kurpiewski, A. 1997, A&A, 326, 419

Krolik, J. H. 1998, ApJ, 498, L13

Kuncic, Z., Celotti, A., & Rees, M. J. 1997, MNRAS, 284, 717

Kusunose, M., & Mineshige, S. 1992, ApJ, 392, 653

Kusunose, M., & Mineshige, S. 1995, ApJ, 440, 100

Kusunose, M., & Zdziarski, A. A. 1994, ApJ, 422, 737

Landau, L. D., & Lifshitz, E. M. 1987, Fluid Mechanics, New York: Pergamon

Lasota, J.-P. 1994, in Theory of Accretion Disks-2, W.J. Duschl, J. Frank, F. Meyer, E. Meyer-Hofmeister, & W.M. Tscharnuter NATO ASI Ser. C, 417, Dordrecht: Kluwer, 341

Liang, E. P. 1979a, ApJ, 231, L111

Liang, E. P. 1979b, ApJ, 234, 1105

Liang, E. P., & Wandel, A. 1991, ApJ, 376, 746

Lightman, A. P., & Eardley, D. M. 1974, ApJ, 187, L1

Magdziarz, P., & Zdziarski, A. A. 1995, MNRAS, 273, 837

Misner, C. W., Thorne, K. S., & Wheeler, J. A. 1973, Gravitation (San Francisco: Freeman)

Nakamura, K. E., Kusunose, M., Matsumoto, R., & Kato, S. 1997, PASJ, 49, 503

Narayan, R. 1992, ApJ, 394, 261

Narayan, R. 1996, ApJ, 462, 136

Narayan, R., Kato, S., & Honma, F. 1997, ApJ, 476, 49

Narayan, R., Mahadevan, R., & Quataert, E. 1998, in Theory of Black Hole Accretion Disks, M. A. Abramowicz, G. Björnsson, & J. E. Pringle, Cambridge: Cambridge Univ. Press

Narayan, R., & Yi, I. 1994, ApJ, 428, L13

Novikov, I. D., Thorne, K. S. 1973, in Black Holes, C. de Witt & B. S. de Witt, New York: Gordon & Breach, 343

Paczyński, B., & Bisnovatyi-Kogan, G. S. 1981, Acta Astron., 31, 3

Paczyński, B., & Wiita, P. J. 1980, A&A, 88, 23

Page, D. N., & Thorne, K. S., 1974, ApJ, 191, 499

Peitz, J., & Appl, S. 1997, MNRAS, 286, 681

Pietrini, P., & Krolik, J. H. 1995, ApJ, 447, 526

Piran, T. 1978, ApJ, 221, 652

Popham, R., & Gammie, C. F. 1998, ApJ, 504, 419

Poutanen, J. 1998, in Theory of Black Hole Accretion Disks, M. A. Abramowicz, G. Björnsson, & J. E. Pringle, Cambridge: Cambridge Univ. Press, 100

Poutanen, J., Krolik, J. H., & Ryde, F. 1997, MNRAS, 292, L21

Poutanen, J., & Svensson, R. 1996, ApJ, 470, 249

Pozdnyakov, L. A., Sobol, I. M., & Sunyaev, R. A. 1979, Sov. Astron. Lett., 5, 279

Pringle, J. E. 1976, MNRAS, 177, 65

Pringle, J. E. 1981, ARA&A, 19, 137

Quataert, E., & Gruzinov, A. 1998, ApJ, submitted (astro-ph/9803112)

Rees, M. J., Begelman, M. C., Blandford, R. D., & Phinney, E. S. 1982, Nature, 295, 17

Riffert H., & Herold H., 1995, ApJ, 450, 508

Ross, R. R., Fabian, A. C., & Young, A. J. 1998, MNRAS, submitted

Rybicki, G. B., & Lightman, A. P. 1979, Radiative Processes in Astrophysics, New York: Wiley

Shakura, N. I. 1972, Soviet Astron., 16, 756

Shakura, N. I., & Sunyaev, R. A. 1973, A&A, 24, 337

Shakura, N. I., & Sunyaev, R. A. 1976, MNRAS, 175, 613

Shapiro, S. L., Lightman, A. P., & Eardley, D. M. 1976, ApJ, 204, 187

Spitzer, L. Jr. 1962, Physics of Fully Ionized Gases, 2d. rev. ed., New York: Interscience

Stern, B. E., Poutanen J., Svensson, R., Sikora, M., & Begelman, M. C. 1995, ApJ, 449, L13

Svensson, R. 1986, in IAU Colloq. 89, Radiation Hydrodynamics in Stars and Compact Objects, D. Mihalas & K.-H. Winkler, New-York: Springer, 325

Svensson, R. 1996, A&AS, 120, 475

Svensson, R., & Zdziarski, A. A. 1994, ApJ, 436, 599

Szuszkiewicz, E., Malkan, M. A., & Abramowicz, M. A. 1996, ApJ, 458, 474

Witt, H. J., Czerny, B., & Życki, P. T. 1997, MNRAS, 286, 848

Woźniak, P. R., Zdziarski, A. A., Smith, D., Madejski, G. M., & Johnson, W. N. 1998, MNRAS, 299, 449

Zdziarski, A. A. 1998, MNRAS, 296, L51

Zdziarski, A. A., Johnson, W. N., Poutanen, J., Magdziarz, P., & Gierliński, M. 1997, in The Transparent Universe, C. Winkler, T. J.-L. Courvoisier, & Ph. Durouchoux, ESA SP-382, Noordwijk: ESA, 373

Zdziarski, A. A., Lubiński, P., & Smith, D. A. 1999, MNRAS, in press

Zdziarski, A. A., Poutanen, J., Mikołajewska, J., Gierliński, M., Ebisawa, K., & Johnson, W. N. 1998, MNRAS, 301, 435

Życki, P. T., Done, C., & Smith, D. A. 1998, ApJ, 496, L25